Original Paper

Cellular Physiology and Biochemistry

Cell Physiol Biochem 2010;25:367-378

Accepted: February 12, 2010

KCNQ1 K^+ Channels are Involved in Lipopolysaccharide-induced Apoptosis of Distal Kidney Cells

Christophe Duranton, Isabelle Rubera, Sebastien L'hoste, Marc Cougnon, Philippe Poujeol, Jacques Barhanin and Michel Tauc

CNRS-FRE 3093, Transport ionique, Aspects normaux et pathologiques Université de Nice-Sophia Antipolis, Nice

Key Words
Potassium channel • Kidney • Patch-clamp • Apoptosis • Endotoxin

Abstract
Most bacteria initiate host inflammatory responses through interactions with epithelial cells. Lipopolysaccharide (LPS), a component of the bacterial cell wall is a major cause of septic shock in emergency care units and in the pathogenesis of acute renal failure. Kidney cells exposed to LPS undergo apoptotic changes, including cell volume decrease, phosphatidylserine exposure, caspase-3- and membrane K^+ conductance -activation. Whole-cell configuration was used to identify K^+ channels in primary and immortalized culture of mice distal convoluted tubules. LPS exposure induced a 3 fold increase in intracellular cAMP concentration and the activation of an outwardly rectifying K^+ conductance in both immortalized and primary culture of distal cells. This LPS-induced current exhibited KCNQ1 K^+ channel characteristics, i.e. inhibition by quinidine, chromanol293B and low dose of HMR1556 (IC50<1 μM) and insensitive to TEA and charybdotoxin. The background-like biophysical properties of the current suggest that the KCNQ1 pore-forming subunit is associated with a KCNE2 or KCNE3 ancillary subunit. RT-PCR experiments confirmed the presence of KCNQ1 and KCNE3 mRNA transcripts in primary culture of distal segments. Activation of the KCNQ1/KCNE3 K^+ current appeared to be an essential step in the LPS-induced apoptosis process since HMR1556 blocked the LPS-induced- cell volume decrease, -caspase-3 activation and -phosphatidylserine exposure.

Introduction

Sepsis is a major cause of mortality in Europe and North America in intensive care units. It is defined as the body's systemic inflammatory response to infection provoked by pathogens or their components such as lipopolysaccharides (LPS). LPS is a component of the gram-negative bacterial cell wall and is a major cause of endotoxemia. LPS has also been implicated in the elaboration of the inflammatory response (secretion of cytokines) and the pathogenicity of the acute renal disease (ARF). *In vivo*, LPS injection can cause a catastrophic disruption of renal cortical peritubular perfusion and renal

KARGER
Fax +41 61 306 12 34
E-Mail karger@karger.ch
www.karger.com

1015-8987/10/0255-0367$26.00/0

Accessible online at:
www.karger.com/cpb

Christophe Duranton
CNRS-FRE 3093, Transport ionique, Aspects normaux et pathologiques
Université de Nice-Sophia Antipolis
06108 Nice Cedex 2 (France)
Tel. +334 92 07 68 94, Fax +334 92 07 68 50, E-Mail duranton@unice.fr

failure [1, 2]. However, LPS-induced hypotension and impairment of oxygen delivery are probably not essential since a model of sepsis was described [3, 4] in which a single injection of LPS leads to ARF with no hemodynamic effects and no alteration of the kidney structure. This separation between severe kidney dysfunction and the absence of modification of the tubular organization can be explained (at least for a significant part) by the increase of apoptotic cell death in the kidney. Interestingly, *in vivo* experiments have shown that caspase inhibitor (Z-VAD) injection preserved renal cortical perfusion, prevented apoptosis, and protected against renal failure [1].

Renal distal tubular epithelial cells are in large part responsible for the regulation of sodium, chloride, and potassium homeostasis in the body. The distal tubule has key paracrine and autocrine functions in secreting an array of inflammatory, reparative and survival signalling molecules that include cytokines, polypeptide growth factors and vasoactive peptides. Interestingly while proximal cells are probably exposed to circulating LPS during sepsis, distal convoluted tubules and collecting ducts represented also target sites for uropathogenic bacteria that cause severe renal interstitial damaged and renal insufficiency. Uropathogenic E. coli have been widely used to test the host-pathogen interactions between bacteria and epithelial cells and there is some evidence that epithelial renal tubule cells participate in the induction of the innate immune response [5].

Ion homeostasis perturbations have been described as important steps in apoptotic program cell death. Importantly, blockage of K^+ efflux by K^+ channel inhibitors prevents the apoptotic process in various cell types [6, 7-9] as well as in cells originated from the proximal tubule [10]. These findings suggest that K^+ channel activation is an essential step in the cascade of events leading to cell apoptosis. The activation of K^+ channels during apoptosis is generally associated with the activation of Cl^- permeability which finally drives water efflux. Altogether, loss of KCl and water leads to a well described normotonic cell volume decrease called Apoptotic Volume Decrease (AVD). Recently, a K^+ channel (TASK2), mainly involved in the regulatory volume decrease (RVD, [11]) of the kidney proximal cells, has been shown to also control the apoptotic volume decrease [10].

Previous experiments performed on human monocytes, macrophages [12, 13] endothelial cells [14, 15] or lung pericytes [16] have clearly established that specific potassium channels are involved in the LPS-mediated cell activation. However, most of these studies provided evidence for a transcriptional regulation of the K^+ channels membrane density. In sharp contrast, elegant studies performed on macrophages [17] and vascular smooth muscle [18] by using single-channel patch-clamp experiments clearly showed that maxi K^+ channel activation can occur in a transcriptional-independent process. Both studies finally conclude that modulation of K^+ channel activity is an early step in the LPS-induced transmembrane signal transduction.

In this study we demonstrate the essential role of K^+ channels activation in the LPS-induced apoptotic process in murine distal tubule kidney cells. Moreover, we found that the K^+ channels activated by LPS are made of the KCNQ1 and KCNE3 subunits and that their activation is mediated by an elevation of cAMP levels through cyclo-oxygenases activation.

Materials and Methods

Primary culture of distal cells

The primary cell culture technique has been described in detail previously [19]. Briefly, C57Bl/6 mice were used to obtain primary culture of distal segments of the nephron. Kidneys were perfused with Hanks' solution containing collagenase (700 kU/l, Worthington, UK). Kidneys were incubated in the presence of collagenase (160 kU/l, 1h) and individual nephrons were then dissected by hand under binoculars and sterile conditions. The criteria used to identify the distal convoluted tubule (DCT) have been described in detail previously [20]. The dissected tubules were transferred to Petri dishes filled with defined culture medium [19] (DMEM-F12, Sigma, Saint Quentin Fallavier, France). Cultured distal cells were used for experiments during a period of 10 days after a minimum of 10 days of culture.

Transformation of primary distal cultures with pSV3 neo and culture protocol

Ten-day-old primary cultures of distal segments were transfected with pSV3 *neo* using lipofectin (Invitrogen). After 48 h, selection of the clones was performed by the addition of G418 (500 µg/ml). Culture medium (DMEM-F12) with the same composition as used for distal primary culture supplemented with G418 (250 µg/ml) was used. Resistant clones were isolated, sub-cultured and used after 10 trypsinization steps.

Annexin-V-FITC and Propidium iodide labeling of distal cells

Apoptosis induced the alteration of the plama membrane with translocation of phosphatidylserine from the inner part of the plasma to the outer layer. PS exposure can be specifically recognized by annexin-V proteins. This property was used to quantify the apoptosis level in distal cells. For this purpose, cell were grown in 35-mm petri dishes and maintained for 24h in freeserum medium. The cells were then exposed to different treatments and co-labelled (Apoalert annexin-V apoptosis kit,

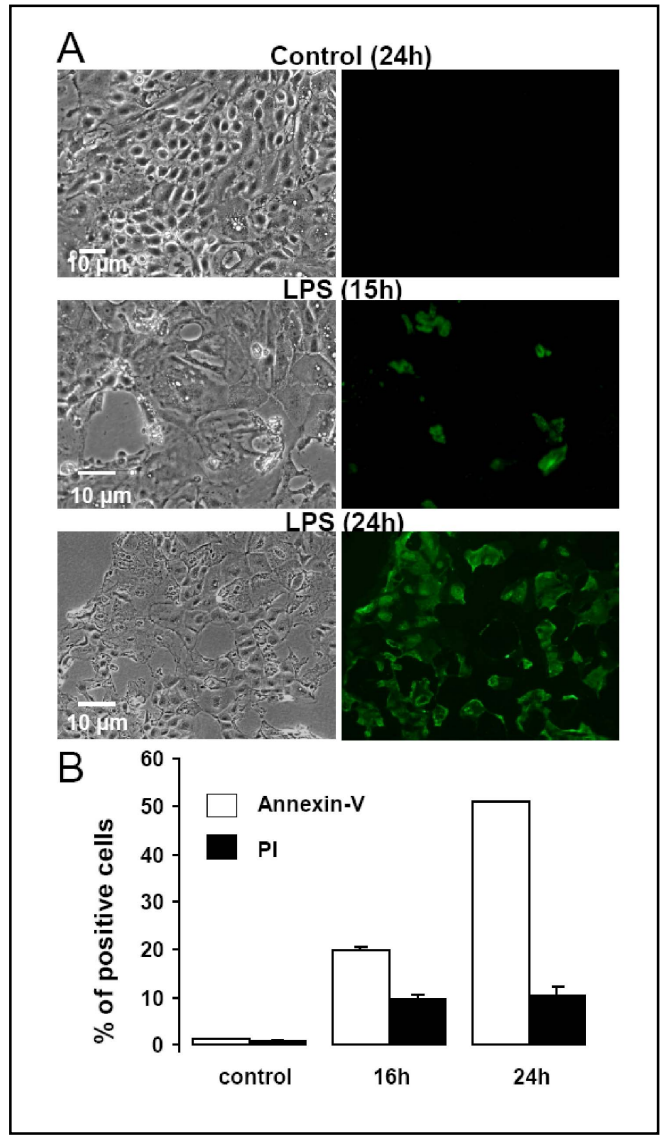

Fig. 1. The endotoxin LPS induces phosphatidylserine exposure and cell death with apoptotic features in primary culture of distal convoluted tubule (DCT). A. Primary culture of distal cells (10-14 days old) from mice were maintained in serum free medium for 15 and 24h in the absence (control) or in the presence of LPS (10 µg/ml). Exposure of phosphatidylserine residues on the outer leaflet of the plasma membrane of the apoptotic cells are stained with the annexin-V FITC. Cells were visualized with a microscope in normal light mode (left) or at 550 nm in the fluorescent mode (right). Given images obtained in normal light and in fluorescent mode correspond to the same field of the monolayer. B. Histograms representing the percentage of annexin- (open bars) and propidium iodide PI- (closed bars) positive cells measured in control condition and after 15 and 24 hours of incubation with LPS (10 µg/ml). Values are means ± SEM of 4 different experiments (3 different micrographs were taken and used for quantifying the annexin or PI positive cells for each primary culture).

Clontech) with annexin-V-FITC conjugate (final concentration: 0.8 µg/ml; 15 min) and propidium iodide (PI, 1 µg/ml). The cells were observed under a fluorescence microscope using a filter set for FITC (550 nm) and PI (585 nm). Apoptotic cells were counted by comparing the 2 staining. A cell was considered apoptotic only if the nucleus was not stained by PI and stained by annexin-V. The numbers of cells positive for annexin-V- or PI-staining were expressed as the percentage of total cells. 3 fields containing around 200 cells each were randomly taken and used to count the number of positive cells for AnnexinV-FITC and/or PI.

Measurement of Caspase-3 activity

Caspase-3 activity was measured using colorimetric assays (CaspACE™ assay system, colorimetric, Promega). The activity was assayed in triplicate or quadruplicate on protein extracts obtained after lysis of distal cell line. The absorbance was measured at 405 nm using an Automated Microplate Reader ELX-800 (Bio-Tek instruments, INC).

Electrophysiological Studies

Whole cell currents were recorded from primary or immortalized cultured cells grown on collagen-coated supports (35mm Petri dishes) maintained at 37°C. The patch pipettes (2- to 4-MΩ) were connected via an Ag-AgCl wire to the head stage of a patch amplifier (RK-400, Biologic, France). The membrane was ruptured by suction to achieve the conventional whole cell configuration. The offset potentials between both electrodes were zeroed before sealing, and the liquid junction potential was corrected accordingly. Voltage-clamp commands, data acquisition, and data analysis were controlled via the RK-400 amplifier. The whole-cell currents resulting from voltage stimuli are sampled at 2.5 kHz and filtered at 1 kHz. Cells were held at -50 mV, and 400 ms pulses from -100 to +100 mV were applied in 20 mV increments. The pipette solution contained (in mM): 140 K-gluconate, 10 HEPES (pH 7.4 adjusted with KOH), 10 EGTA, 1 $CaCl_2$ (free calcium concentration of 10 nM) and 2-5 MgATP (Pos = 290 mosmol/kg H_2O). To avoid spontaneous activation of volume-sensitive K^+ currents, the bath solution was slightly hyperosmotic and contained (in mM): 145 K-gluconate, 10 HEPES (pH 7.4 adjusted with KOH), 5 glucose, 1 $CaCl_2$, 1 $MgCl_2$ and mannitol (Pos = 320 mosmol/kg H_2O).

Measurements of intracellular cAMP concentration

cAMP intracellular concentration measurements were performed using a cAMP competitive enzyme immunoassay kit (Sigma). Distal cell line cultured 24 h in serum free culture medium were exposed to LPS (10 µg/ml) and lysed with HCl (0.01 N, 10 min at 4°C). The cAMP concentration of each sample was measured using colorimetric assays according to the protocol provided by the manufacturer.

Cell volume measurement

Cell volume was measured by an electronic sizing technique using a CASY 1 cell counter (SCHÄRFE SYSTEM®).

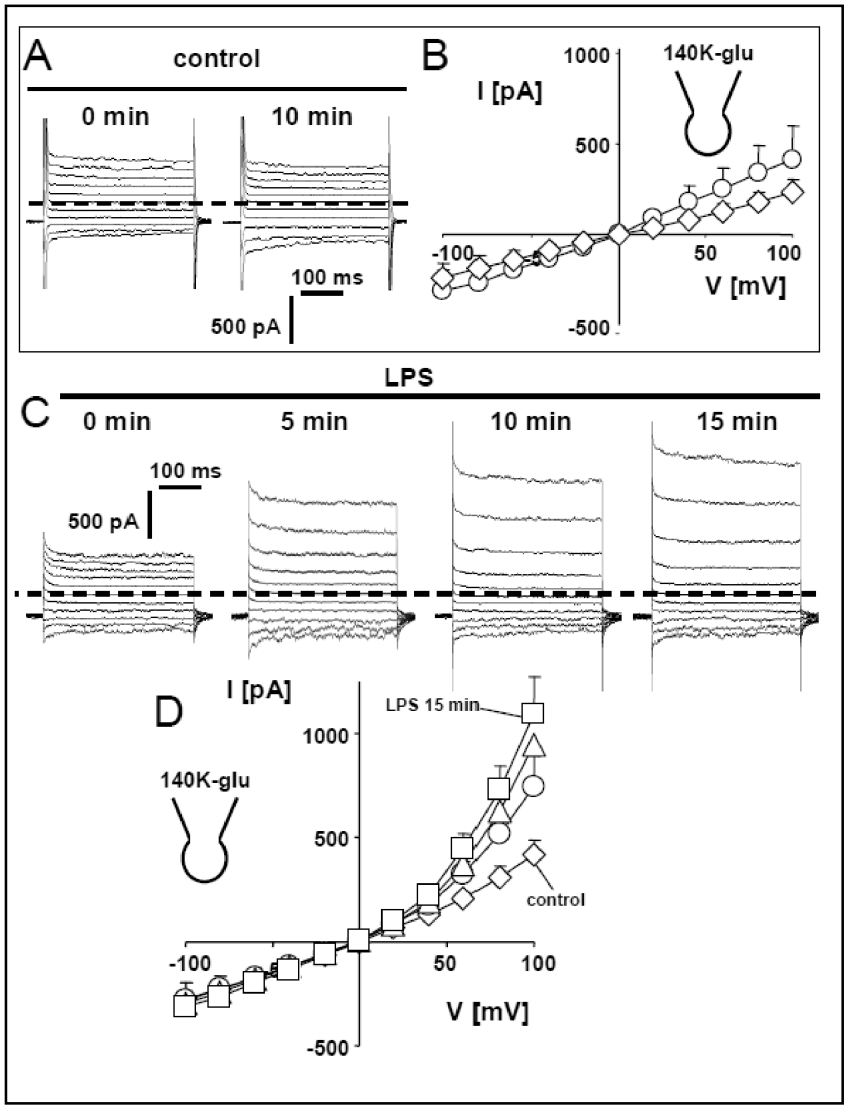

Fig. 2. Effect of the endotoxin (LPS) on the development of K^+ currents in primary culture of mouse DCT cells. A. Whole-cell current traces recorded in control condition just after achievement of the whole-cell configuration (left) and 10 min after (right). Records were performed with symmetrical K-gluconate pipette and bath solution. Currents were obtained in fast whole-cell voltage-clamp mode. The membrane potential was held at -50 mV and currents were elicited by a train of 11 voltage steps (400 ms duration) between -100 and +100 mV; zero current is indicated by dashed line. B. Mean current-voltage (I/V) relations (± SEM, n=4 from 4 different monolayers) of DCT cells recorded as in (A) in control condition just after achievement of the whole-cell configuration (circles) and 10 minutes after (squares). Current values were analyzed between 350 and 375 ms of each square pulses. C. Whole-cell current traces recorded before (control) and after addition (5, 10 and 15 min) of LPS (10 µg/ml) to the K-gluconate bath solution. The pipette was filled with the standard K-gluconate pipette solution. Zero current is indicated by dashed line. D. Mean I/V-relations (± SEM, n=12 cells from 12 different monolayers) recorded as in (C) in control condition (diamonds), 5 min (circles), 10 min (triangles) and 15 min after LPS exposure (10 µg/ml; squares). Values are means ± SEM.

Immortalized distal cells were exposed to different treatments for 24h rapidly trypsinized (1X), and cell volume measurements were performed just after by suspending the cells in casyton® solution. A minimum of 30,000 cells were measured in triplicate for each experimental conditions.

RT-PCR

Total RNA was prepared from 10-day-old primary cultures of distal tubules dissected from wild type kidney mice using an RNeasy Mini Kit (QIAGEN). cDNA synthesis was carried out using Superscript First-Strand Synthesis System for RT-PCR (Invitrogen) according to the manufacturer's instructions. The following oligonucleotide primers were used to amplify kcnq1 (420 bp) and kcne3 (300 bp): kcnq1 sense: 5'-CCC TCT TCT GGA TGG AGA-3', kcnq1 antisense: 5'-ATC TGC GTA GCT GCC AAA-3', annealing temperature, Ta 54°C; kcne3 sense: 5'-AAC GGG ACT GAG ACC TGG TA-3', kcne3 antisense 5'-CAT CAG ATC ATA GAC ACA CGG-3', Ta 58°C. PCR conditions were 35 cycles of 30 s at 94°C, 30 s at Ta and 30 s at 72°C.

Chemical Compounds

LPS (E. coli O111:B4, Invivogen, USA) was prepared in an ethanol/pyrogen-free distilled water mixture (1/5 volume, stock solution 10 mg/ml) and stored at 4°C for one month. LPS stock solution was then diluted at a final concentration of 10 µg/ml. TEA and quinidine (Sigma) were prepared directly at the final concentrations. Chromanol 293B (Sigma) and HMR1556 (provided by Dr Gerlach U, Aventis to JB) were dissolved in DMSO at final concentration of 100 mM and 10 mM respectively. H89 and indomethacin (Sigma) were prepared in DMSO (stock solution 10 mM) and used at a final concentration of 10 µM.

Results

The loss of asymmetric distribution of phosphatidylserine (PS) in the cell membrane is known to be an early phenomenon during the cascade of events

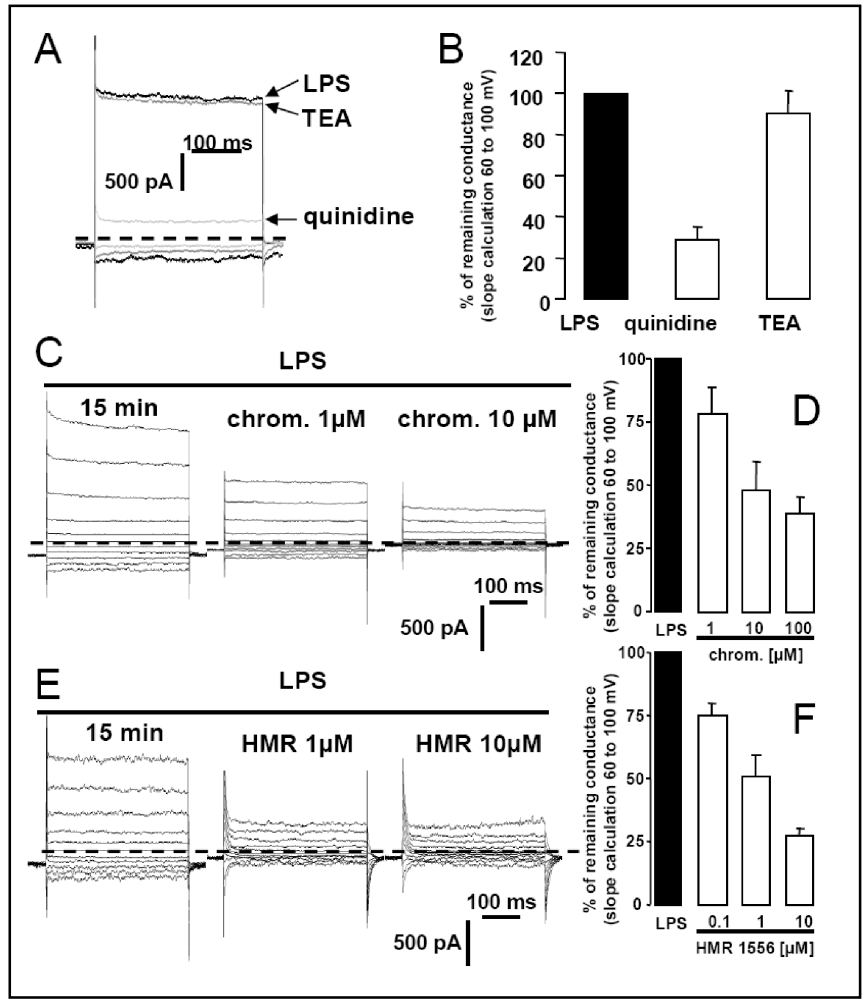

Fig. 3. Sensitivity of the LPS-induced K^+ current to K^+ channels blockers in primary culture of mouse DCT cells. A. Whole-cell current traces recorded 15 min after LPS exposure illustrating the sensitivity of the LPS-induced K^+ currents to TEA (1 mM) and quinidine (500 µM). The membrane potential was held at -50 mV and currents were elicited by 2 square pulses (400 ms duration) at -100 and +100 mV. Records were performed with symmetrical K-gluconate pipette and bath solution. Zero current is indicated by dashed line. B. Inhibition of the LPS-induced K^+ currents by quinidine and TEA. The percents of inhibition were calculated by comparing the conductance (calculated between 60 and 100 mV) in the presence of quinidine (500 µM, n=5) or TEA (1 mM, n=4) versus that obtained before addition of the inhibitors (LPS). Values are means ± SEM. C. Whole-cell current traces recorded 15 min after LPS exposure in the absence (left) or presence of increasing concentrations of chromanol 293B (1-10 µM). Records were performed with symmetrical K-gluconate pipette and bath solution. The membrane potential was held at -50 mV and currents were elicited by a train of 11 voltage steps (400 ms duration) between -100 and +100 mV. D. Dose dependent inhibition of chromanol 293B on the LPS-induced K^+ currents. The percents of inhibition were calculated by comparing the conductance measured in the presence of LPS (calculated between 60 and 100 mV after 15 min of LPS exposure) to the conductances measured in the presence of increasing concentrations of chromanol (1, 10 and 100 µM). Values are means ± SEM of 6 cells (5 different monolayers). E. Whole-cell current traces recorded 15 min after LPS exposure in the absence (left) or presence of increasing concentrations of HMR-1556 (1-10 µM). Records were performed with symmetrical K-gluconate pipette and bath solution. Zero current is indicated by dashed line. F. Dose dependent inhibition of HMR-1556 on the LPS-induced K^+ currents. The percents of inhibition were calculated by comparing the conductance measured in the presence of LPS (calculated between 60 and 100 mV after 15 min of LPS exposure) to the conductances measured in the presence of increasing concentrations of HMR-1556 (0.1, 1 and 10 µM). Values are means ± SEM of 5 cells (5 different monolayers).

leading to apoptosis. To test whether LPS induced PS redistribution at the outer leaflet of the plasma membrane, primary culture of mouse DCT cells (15-21 days old) were exposed to LPS (10 µg/ml) for 15 and 24 h and stained with annexin-V-FITC (Fig. 1A) and propidium iodide (PI) to control the membrane integrity. In control condition, the culture appears as an homogenous epithelium composed of juxtaposed cells all negative for annexin and PI labelling. By contrast, epithelium exposed to LPS (15h, 10 µg/ml) display profound modifications of the epithelium integrity with apparition of regions without cells. Some cells were bright and condensed and positively stained by annexin-V-FITC. After a 24h-LPS incubation, the fraction of condensed cells positively stained by annexin-V-FITC was significantly increased as compared to 15h treatment. Fig. 1B illustrated the percent of annexin-V and PI positive cells recorded after 15 and 24 hours of LPS exposure. The percentage of annexin positive cells rose from 1 ± 1 % in control condition to 20 ± 1 % and 51 ± 1 % after 15 and 24h of LPS exposure, respectively. At the same LPS exposure times the percentage of PI positive cells increased from 1 ± 1 %

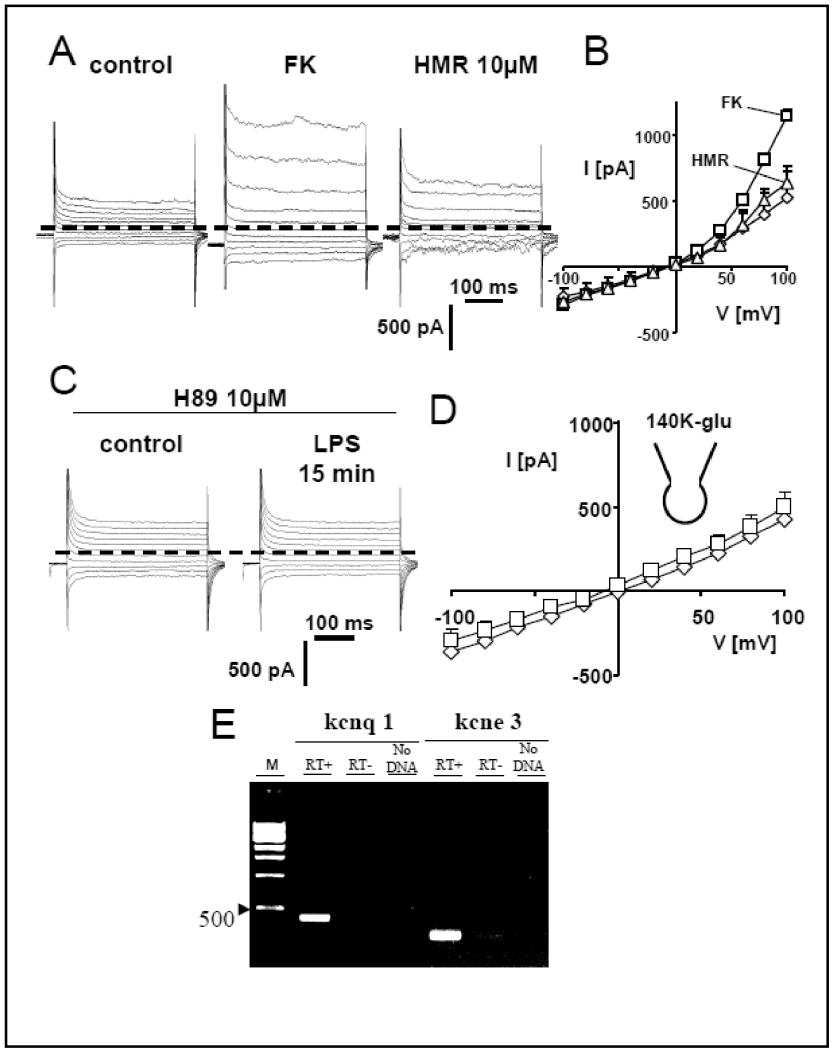

Fig. 4. Sensitivity of the forskolin-induced K^+ conductance to HMR-1556 and effect of H89 on the LPS-induced K^+ current in primary culture of mouse DCT cells. A. Whole-cell current traces recorded in control condition and 10 min after forskolin exposure (10 µM, 10 min) and finally after addition of HMR-1556 to the K-gluconate bath solution. Zero current is indicated by dashed line. B. Mean I/V-relations (± SE, n=4 cells from 4 different monolayers) recorded as in (A) in control condition (diamonds), after 10 min of forskolin exposure (squares) and in the presence of HMR-1556 (10 µM, triangles). Values are means ± SEM. C. Whole-cell current traces illustrating the effect of H89 (10 µM, pre-incubation of 30 min) on the development of the LPS-induced conductance. DCT cells were pre-incubated for 30-45 min in the presence of H89 and recorded before (control, left) and after 15 min of LPS exposure (10 µg/ml, right). Zero current is indicated by dashed line. Mean I/V-relations recorded as in (C) after a 30 min pre-incubation with H89 (10 µM, diamonds) and then after 15 min of LPS stimulation (squares). Values are means ± SEM of 7 cells from 7 different monolayers. D. RT-PCR determination of kcnq1 mRNA and kcne3 mRNA in primary cultures of distal tubules obtained from wild type mice. RT-PCR analysis was performed with primers specific for kcnq1 or kcne3. RT-PCR was performed in the presence (RT+) or the absence (RT-) of reverse transcriptase to control for DNA contamination. M: markers.

(control) to 9 ± 3 (15h) and 10 ± 2 % (24h). Similar observations were also obtained in an immortalized DCT cell line (not shown). These experiments indicated that LPS induced exposure of PS residues on the outer l eaflet of the plasma membrane in primary culture and in cell line originating from DCT segments.

Patch-clamp whole-cell experiments were performed in primary culture of DCT cells to test the ability of LPS to activate K^+ currents. Fig. 2A illustrates the K^+ currents recorded in DCT cells in control conditions, the voltage step protocol elicited small currents that were not significantly modified after 10 min of recording. The corresponding I/V curve (Fig. 2B) indicated a reversal potential close to 0 mV and a maximal slope conductance (calculated between +80 and +100 mV) of 4.1 ± 1.6 nS (n=5) at the beginning of the experiment (0 min) and of 2.9 ± 0.9 nS after 10 min of recording. By contrast, LPS exposure (10 µg/ml) induced a time-dependent increase of the outward currents, with a maximal activation observed at 15 min of incubation (Fig. 2C). The slope conductance was 5.0 ± 0.9 nS (n=11) at the beginning of the experiment and reached 16.6 ± 2.7 nS (n=11) after 15 min of LPS exposure (Fig. 2D).

We next examined the sensitivity of the LPS-induced K^+ current to various K^+ channels inhibitors. Quinidine (500 µM) reduced by more than 70 % the LPS-induced current recorded at +100 mV (Fig. 3A-3B) but TEA and charybdotoxin (data not given) have no effects. Interestingly, chromanol-293B (an inhibitor of KCNQ1 channel) induced a dose-dependent inhibition of the LPS-induced K^+ current (Fig. 3C-D). 10 µM of chromanol reduces by more than 50 % the LPS-induced conductance. A significant inhibition of LPS-induced channel was also obtained with the chromanol derivative HMR-1556 (Fig. 3E-F). The low IC_{50} for HMR1556 (< 1 µM) suggest the involvement of KCNQ-1/KCNE-3 association rather than KCNQ-1 alone. The KCNE-3 subunit is known to modulate the KNCQ-1 channel

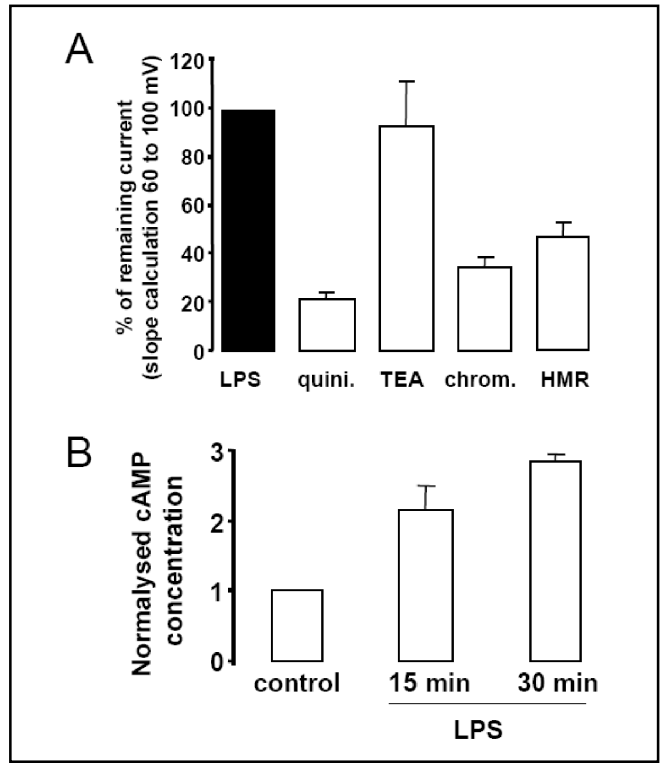

Fig. 5. Effect of LPS on the development of K^+ currents and intracellular cAMP concentration in immortalized mouse DCT cells. A. Percent of inhibition of the LPS-induced K^+ currents in the presence of quinidine, TEA, chromanol 293B and HMR-1556 in DCT cell line. The percents of inhibition were calculated by comparing the conductance (calculated between 80 and 100 mV) measured in the presence of quinidine (500 µM, n=5), TEA (1 mM, n=4), chromanol 293B (10 µM, n=5) and HMR-1556 (10 µM, n=5) versus that obtained before addition of the inhibitors (LPS, 10 min 10 µg/ml). Values are means ± SEM. B. Variations of cAMP intracellular concentration during LPS exposure. Immortalized DCT cells were seeded in collagen coated petri dishes and grown 48 hours to reach a confluence of 60-80 %. The cells were then exposed to LPS (10 µg/ml) for 15 and 30 min. Cells were lysed and the intracellular concentration of cAMP was measured using a competitive enzyme immunoassay kit. The concentration of intracellular cAMP for each time points is normalized to the value recorded in absence of LPS (control). Values are means ± SEM of 5 independent experiments.

activity when the intracellular cAMP concentration increases. A previous study [19] has identified a K^+ conductance activated by forskolin (FK) and inhibited by chromanol in cells originating from DCT. It was then of interest to verify if 1/the FK-activated K^+ current is inhibited by low dose of HMR-1556 and 2/if the inhibitor of cAMP-dependent PKA (H89) prevented the LPS-induced K^+ current.

As a result the FK-activated K^+ current is significantly inhibited by HMR-1556 (Fig. 4A). The corresponding I/V curves (Fig. 4B) indicated a maximal slope conductance (calculated between +80 and +100 mV) of 5.3 ± 1.3 nS (n=3) in control condition which increased to 16.3 ± 1.3 nS after FK exposure. The addition of 10 µM of HMR-1556 reduced the maximal slope conductance to 6.8 ± 1.6 pS. Moreover, when DCT cells are pre-incubated with H89 (10 µM, 30 min), LPS (10 µg/ml) failed, in all the tested cells (n=7), to stimulate a K^+ conductance (Fig 4. C, D). The identification by RT-PCR of amplified products for KCNQ1 and KCNE3 confirmed the presence of mRNA encoding for both proteins in primary culture (15 day-old) of DCT segments (Fig. 4E) and supported the hypothesis of a KCNQ1/KCNE3 mediated LPS-induced apoptosis.

The activation of K^+ current by LPS exposure was also tested in DCT cell line immortalized from primary cultures. As expected, LPS (10 µM) induced a significant increase of the maximal slope conductance from 13.4 ± 2.0 nS (n=19) in control condition to 31.3 ± 6.6 nS after LPS exposure (data not shown). Fig. 5A illustrated the percent of remaining currents recorded at +100 mV after LPS exposure in the presence of various inhibitors. The LPS-induced K^+ currents recorded in DCT cell line shared similar sensitivity to quinidine, Chromanol-293B (10µM) and HMR1556 as compared to the K^+ current recorded in the cells obtained by primary culture of DCT. The LPS-induced current remained insensitive to TEA or ChTX (not given).

Altogether, these data suggested that KCNQ1 channels are also activated in DCT cell line. The involvement of KCNE-3 subunit suggested a regulation of the channel activity by intracellular variations of cAMP. Thus, cAMP intracellular concentration was monitored in the absence (control condition) and in the presence of LPS or FK (Fig. 5D). LPS induced a ~2 and ~3 fold increase of intracellular cAMP concentration when incubating the DCT cells for 15 and 30 min, respectively. FK (10 µM, 20 min, not shown), increase by ~18 fold the intracellular cAMP concentration. In conclusion, LPS activates probably KCNQ1/KNCE3 channel complex by increasing the intracellular cAMP concentration which in turn generate efflux of K^+.

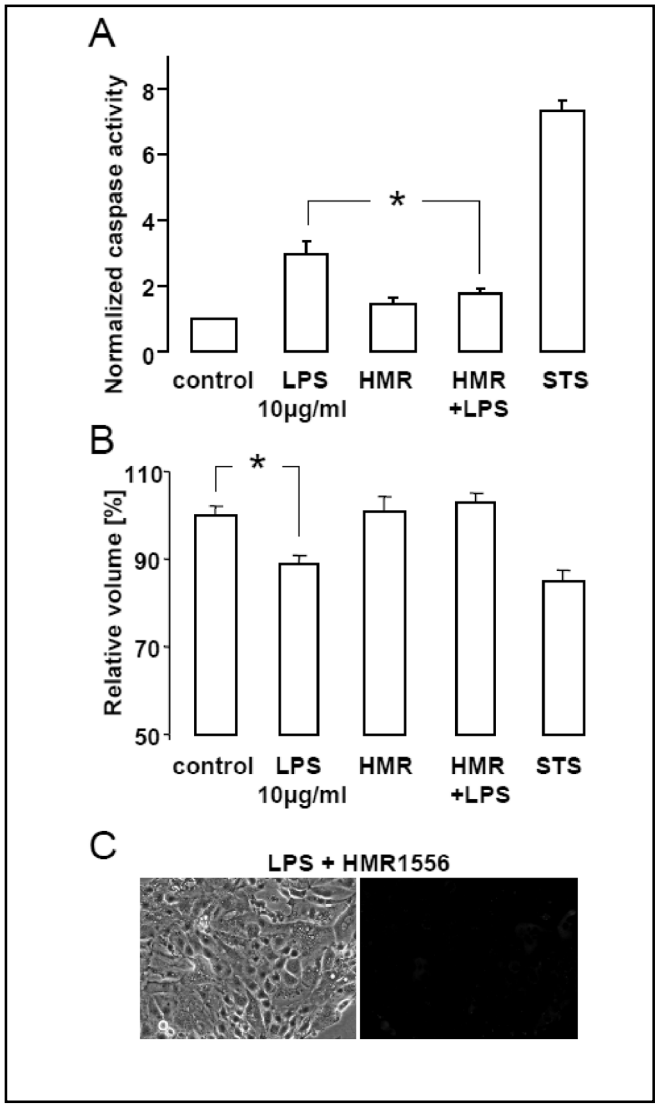

Fig. 6. Effects of HMR-1556 on the LPS-induced apoptosis in immortalized mouse DCT cells. A. Normalized caspase-3 activity measured in distal cells line in control condition, in the presence of LPS (10 µg/ml, 24h), HMR-1556 (10 µM) or concomitant presence of both substances (LPS+HMR, 24h). A positive control was performed by exposing distal cell line to staurosporine (STS, 1 µM) for 6 hours. Values are means ± SEM of 4 -5 independent cell cultures. *, $p < 0.05$; Student's *t* test. B. Normalized cell volume variations measured in immortalized distal cells in control conditions, in the presence of LPS (10 µg/ml, 24h), HMR-1556 (10 µM, 24h) or in the concomitant presence of both substances (LPS+HMR, 24h). A positive control was performed by exposing distal cell line to staurosporine (STS, 1 µM, 6 h). Cell volume was measured by an electronic sizing technique with a CASY 1 cell counter (SCHÄRFE SYSTEM®). Values are means ± SEM of 4 different experiments. *, $p < 0.05$; Student's *t* test. C. Primary culture of distal cells (10-12 day-old) from mice were maintained in serum free medium for 15 and 24h in the presence of LPS (10 µg/ml) or concomitant presence of LPS and HMR-1556 (10 µM). Cells were visualized with a microscope in normal light (left) or at 550 nm in the fluorescent mode (right). Given images obtained in normal light and in fluorescent mode correspond to the same field of the monolayer. HMR-1556 abolished the LPS-induced phosphatidylserine exposure in all tested primary cultures (n=6).

To confirm the involvement of the KCNQ1/KNCE3 complex in the apoptosis, caspase-3 activity and the relative cell volume variation were measured in DCT cell line during LPS treatment in the presence of HMR-1556. LPS alone induced after 24h of exposure a significant increase of caspase-3 activity (~3 fold, Fig. 6A) and cell volume reduction (13 ± 2%, Fig. 6B). Interestingly, addition of HMR-1556 completely abolished the LPS induced- capase-3 activation and -cell volume reduction. HMR-1556 alone remained without effect. The apoptotic agent STS induced a significant caspase-3 activation (~7 fold increase) and a reduction of cell volume (15 ± 4%). Taken together these experiments strongly suggested that LPS induced apoptosis in DCT cell line by activating KCNQ1/KNCE3 complex which in turn induced AVD and caspase-3 activation. In a similar way, LPS-exposed DCT cells obtained by primary culture (24 h, 10 µg/ml) and incubated in the concomitant presence of HMR-1556 (10µM) failed to reveal a significant annexin-V-FITC labelling (fig 6C) suggesting that HMR-1556 prevents apoptotic process in DCT cell line as well as in primary culture.

LPS is known to up-regulate COX-2 (cyclo-oxygenase-2) expression in a time-dependent manner resulting in the prostaglandins secretion that causes cellular and humoral responses. To verify that the LPS-induced apoptosis is related to an increase of prostaglandins, whole-cell experiments were performed in distal cells pre-incubated for 30 min in the presence of the non-specific COX inhibitor (indomethacin, 10 µM). Interestingly, none of the pre-treated cells (n=7, Fig. 7A-B) develop a K^+ current when they were exposed to LPS (10 µg/ml, for 15 min). Similarly, the caspase-3 activity (Fig. 7C) was not significantly changed when distal cells were co-incubated for 24h in the presence of indomethacin (10 µM) and LPS (10 µg/ml).

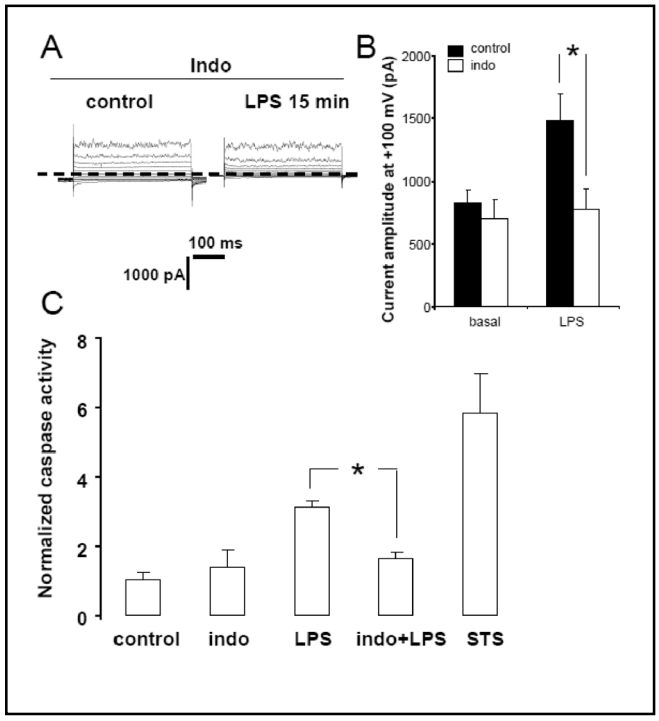

Fig. 7. Effects of indomethacin on the LPS-activated K^+ current and the caspase-3 activity in immortalized mouse DCT cells. A. Whole-cell current traces recorded before (control) and 15 min after addition of LPS (10 µg/ml) to the K-gluconate bath solution. The cells were pre-incubated with indomethacin (10 µM) for 30 min before achievement of the whole-cell configuration. The pipette was filled with the standard K-gluconate pipette solution. Zero current is indicated by dashed line. B. Means of the maximal current amplitude (measured at +100 mV, ± SEM) recorded in immortalized distal cell line before (basal) and 15 min after LPS exposure. The currents were recorded as in (A) in control condition (black bars, n=14) or after an incubation with indomethacin (open bars, 10 µM, 30 min, n=7). *, $p < 0.05$; Student's *t* test. C. Normalized caspase-3 activity measured in distal cells line in control condition, in the presence of indomethacin (10 µM, 24h), LPS (10 µg/ml, 24h) or in the concomitant presence of both substances (indo+LPS, 24h). A positive control was performed by exposing distal cells to staurosporine (STS, 1 µM) for 6 hours. Values are means ± SEM of 4 independent cell cultures. *, $p < 0.05$;, Student's *t* test.

Discussion

Whereas Lipopolysaccharides (LPS) has well-described hemodynamic effects [4], the decrease of the renal function in response to LPS can occur at relatively low dose of LPS that do not produce significant hypotension. Cunningham and colleagues [3] described a model of acute renal failure in which hemodynamic effects of LPS were almost absent despite severe kidney impairment and relatively modest structural tubular injury. A possible explanation for this LPS-hemodynamic-insensitive renal dysfunction and the observed absence of structural kidney damage is apoptotic cell death [1]. The present study confirmed that LPS can induce caspase-3-mediated apoptosis in kidney cells originating from the distal convoluted tubules. Previous *in vitro* experiments have also established that renal epithelial cells exposed to various chemical agents (staurosporine [10], TNFα [3], cyclosporine [10, 21], antitumor platinum derivatives [22-25], cadmium [26-29],or even during pathological situations (ischemia/reperfusion, [30]) are dying through apoptotic processes.

Apoptosis is characterized by a wide variety of events (nuclear condensation, DNA fragmentation, cell shrinkage, mitochondrial depolarization, cytochrome c release, etc.) leading to cell death (see for review [31]) and elimination of potentially harmful cells. It is now admitted that the initial process leading to apoptosis is the apoptotic volume decrease (AVD). A number of studies (see for review [31-33]) have established that the AVD process is driven by loss of cytosolic ions (K^+ and Cl^-), due to the activation of K^+ and Cl^- channels. The present study supports this hypothesis and shows that distal cells undergoing LPS-induced apoptosis are also decreasing their cellular volume. Previous experiments performed on human monocytes, macrophages [12, 13] endothelial cells [14, 15] or lung pericytes [16] have clearly established that K^+ selective potassium channels are involved in the LPS-mediated cell activation. Patch-clamp experiments have even established that maxi K^+ channels activation occurs in a few minutes after LPS exposure [17, 18]. The authors conclude that modulation of K^+ channel activity is an early step in the LPS-induced transmembrane signal transduction.

Interestingly, a number of K^+ channels are known to participate in the AVD process especially in highly differentiated cells: TASK-2 in proximal kidney cells [10]; ROMK1 (Kir1.1) in hippocampal neurons [6] or, maxi-K channels in vascular smooth muscle cells [34]. It was then of interest to characterize the molecular identity of the K^+ channel activated in DCT cells by LPS. Of all the K^+ channels already described in the literature, KCNQ-1 channel was potentially a good candidate to generate the LPS-induced outwardly rectifying K^+ currents. The presence of KCNQ1 channel in the kidney has been demonstrated by RT-PCR [35] and *in situ* hybridization experiments [36]. More recently, experiments have clearly es-

tablished that 1/KCNQ-1 mRNA are present in mouse micro-dissected tubules of the distal and connecting ducts [37] and 2/an intense basolateral labelling of the DCT and CNT using anti-KCNQ1 polyclonal antibody immunolabelling [37]. In the present study, we also confirmed by RT-PCR the presence of KCNQ-1 mRNA transcripts in primary culture of mouse DCT cells. The specific pharmacology of the LPS-induced conductance, with an absence of effect of TEA and ChTX and an inhibition of the conductance by chromanol 293B and HMR-1556 confirmed the involvement of KCNQ-1. Moreover, the low IC_{50} for chromanol 293 B (<10 μM) and HMR1556 (<1 μM) supports also the involvement of KCNQ1/KCNE3 rather than KCNQ1 alone. KCNQ-1 is a delayed voltage-gated channel that enable a K^+ current after electrical depolarization of the cell membrane in the heart [38] KCNQ-1 gene mutations cause in human the Jervell and Lange-Nielsen syndrome characterised by hearing loss and cardiac conduction abnormality [39]. KCNQ-1 alone can generate an outwardly rectifying K^+ current however interactions with beta-subunits (KCNE-1, KCNE-2, KCNE-3) profoundly modify the biophysical properties of the channel [40] and probably its function and role in the target tissue. While KCNQ-1/KCNE-1 association modify the time dependent activation of the current without affecting the amplitude; the beta-subunit KCNE3 markedly changes KCNQ1 properties to an outwardly currents that are nearly instantaneous with an enhanced sensitivity to chromanol 293B (IC50 below 10 μM) and HMR-1556 below (IC50 below 1 μM) [41]. Such sensitivities was observed in the present study for the LPS-induced current. In the literature, it has been demonstrated that KCNE-3 confers a cAMP functional regulation to the KCNQ-1 channel. Interestingly, previous patch-clamp experiments [19] performed in DCT cells have shown that forskolin strongly activated a chromanol 293B-sensitive K^+ conductance supporting the hypothesis of functional KCNQ-1/KCNE-3 association in the DCT. In the present study, the pharmacological sensitivity suggests that the forskolin-activated current and the LPS-induced current are driven by the same type of cAMP-dependent channel (KCNQ-1/KCNE-3). LPS induced in a few minutes (<30 min) a significant increase in intracellular cAMP concentration supporting the hypothesis of cAMP dependent apoptotic process in the DCT cells. Moreover, we have also confirmed by RT-PCR the presence of KCNQ-1 and KCNE-3 mRNA transcripts in primary cells culture of mouse DCT. Involvement of KCNQ-1 channel in apoptosis process has already been proposed for IEC-6 enterocytes cell line [42]. But in this study we demonstrated the involvement of cAMP signalling modulating KCNQ-1/KCNE-3 in the apoptosis process. The inhibition of both LPS-induced-K^+ current and -apoptosis by H89 confirmed the involvement of KCNQ-1/KCNE-3 in this process.

LPS is known to induce multiple intracellular signalling pathways leading to various physiological effects following a paracrine and/or autocrine secretion of cytokines and inflammatory mediators. Beyond the pro-inflammatory mediators, PGE-2, the most prevalent derivative of arachidonic acid is well known to modulate cellular and humoral immune responses. It was then of interest to verify if a putative PGE-2 pathway is related to the LPS-induced apoptosis. As a result, addition of indomethacin to the bath (a non specific inhibitor of cyclo-oxygenases) prevented not only the development of the K^+ current but also the caspase-3 activation and the cell apoptosis. PGE-2 activity is dependent on binding to one of four different G-protein coupled receptors, EP1, EP2, EP3, or EP4 that induce various intracellular coupling mechanisms (for review, see [43]). In the kidney, previous studies have established that EP4 and EP2 receptors are strongly expressed in the DCT segments [44] supporting the hypothesis that cAMP-coupled PGE-2 pathway might exist at this specific nephron segment. Altogether, the inhibition of the cAMP-activated K^+ conductance by indomethacin strongly suggests that LPS induces the production of PGE-2 which stimulates prostanoid receptors that leads to the activation of the cAMP second messenger pathway.

In conclusion, the present study demonstrated the activation of KCNQ-1/KCNE-3 conductance by LPS in DCT cells. This conductance plays a major role in the LPS-induced apoptosis since HMR-1556 (specific inhibitor of KCNQ-1/KCNE-3 channel) abolishes the caspase-3 activation, the cell volume decrease and the PS exposure (3 typical features of apoptosis process). Altogether, this study implicates KCNQ-1/KCNE-3 channel in the LPS-mediated pathogenesis of renal disease during septicaemia and distal segments bacterial retrograde infection.

References

1 Guo R, Wang Y, Minto AW, Quigg RJ, Cunningham PN: Acute renal failure in endotoxemia is dependent on caspase activation. J Am Soc Nephrol 2004;15:3093-3102.

2 Tiwari MM, Brock RW, Megyesi JK, Kaushal GP, Mayeux PR: Disruption of renal peritubular blood flow in lipopolysaccharide-induced renal failure: role of nitric oxide and caspases. Am J Physiol Renal Physiol 2005;289:F1324-1332.

3 Cunningham PN, Dyanov HM, Park P, Wang J, Newell KA, Quigg RJ: Acute renal failure in endotoxemia is caused by TNF acting directly on TNF receptor-1 in kidney. J Immunol 2002;168:5817-5823.

4 Knotek M, Rogachev B, Wang W, Ecder T, Melnikov V, Gengaro PE, Esson M, Edelstein CL, Dinarello CA, Schrier RW: Endotoxemic renal failure in mice: Role of tumor necrosis factor independent of inducible nitric oxide synthase. Kidney Int 2001;59:2243-2249.

5 Patole PS, Schubert S, Hildinger K, Khandoga S, Khandoga A, Segerer S, Henger A, Kretzler M, Werner M, Krombach F, Schlondorff D, Anders HJ: Toll-like receptor-4: renal cells and bone marrow cells signal for neutrophil recruitment during pyelonephritis. Kidney Int 2005;68:2582-2587.

6 Nadeau H, McKinney S, Anderson DJ, Lester HA: ROMK1 (Kir1.1) causes apoptosis and chronic silencing of hippocampal neurons. J Neurophysiol 2000;84:1062-1075.

7 Ekhterae D, Platoshyn O, Zhang S, Remillard CV, Yuan JX: Apoptosis repressor with caspase domain inhibits cardiomyocyte apoptosis by reducing K+ currents. Am J Physiol Cell Physiol 2003;284:C1405-1410.

8 Trimarchi JR, Liu L, Smith PJ, Keefe DL: Apoptosis recruits two-pore domain potassium channels used for homeostatic volume regulation. Am J Physiol Cell Physiol 2002;282:C588-594.

9 Lauritzen I, Zanzouri M, Honore E, Duprat F, Ehrengruber MU, Lazdunski M, Patel AJ: K+-dependent cerebellar granule neuron apoptosis. Role of task leak K+ channels. J Biol Chem 2003;278:32068-32076.

10 L'Hoste S, Poet M, Duranton C, Belfodil R, e Barriere H, Rubera I, Tauc M, Poujeol C, Barhanin J, Poujeol P: Role of TASK2 in the control of apoptotic volume decrease in proximal kidney cells. J Biol Chem 2007;282:36692-36703.

11 L'Hoste S, Barriere H, Belfodil R, Rubera I, Duranton C, Tauc M, Poujeol C, Barhanin J, Poujeol P: Extracellular pH alkalinization by Cl-/HCO3- exchanger is crucial for TASK2 activation by hypotonic shock in proximal cell lines from mouse kidney. Am J Physiol Renal Physiol 2007;292:F628-638.

12 McKinney LC, Gallin EK: Effect of adherence, cell morphology, and lipopolysaccharide on potassium conductance and passive membrane properties of murine macrophage J774.1 cells. J Membr Biol 1990;116:47-56.

13 Vicente R, Escalada A, Coma M, Fuster G, Sanchez-Tillo E, Lopez-Iglesias C, Soler C, Solsona C, Celada A, Felipe A: Differential voltage-dependent K+ channel responses during proliferation and activation in macrophages. J Biol Chem 2003;278:46307-46320.

14 Hoang LM, Chen C, Mathers DA: Lipopolysaccharide rapidly activates K+ channels at the intracellular membrane face of rat cerebral artery smooth muscle cells. Neurosci Lett 1997;231:25-28.

15 O'Brien AJ, Thakur G, Buckley JF, Singer M, Clapp LH: The pore-forming subunit of the K(ATP) channel is an important molecular target for LPS-induced vascular hyporeactivity in vitro. Br J Pharmacol 2005;144:367-375.

16 Burri PH, Djonov V: Intussusceptive angiogenesis—the alternative to capillary sprouting. Mol Aspects Med 2002;23:S1-27.

17 Blunck R, Scheel O, Muller M, Brandenburg K, Seitzer U, Seydel U: New insights into endotoxin-induced activation of macrophages: involvement of a K+ channel in transmembrane signaling. J Immunol 2001;166:1009-1015.

18 Yakubovich N, Eldstrom JR, Mathers DA: Lipopolysaccharide can activate BK channels of arterial smooth muscle in the absence of iNOS expression. Biochim Biophys Acta 2001;1514:239-252.

19 Belfodil R, Barriere H, Rubera I, Tauc M, Poujeol C, Bidet M, Poujeol P: CFTR-dependent and -independent swelling-activated K+ currents in primary cultures of mouse nephron. Am J Physiol Renal Physiol 2003;284:F812-828.

20 Chabardes D, Imbert-Teboul M, Montegut M, Clique A, Morel F: Distribution of calcitonin-sensitive adenylate cyclase activity along the rabbit kidney tubule. Proc Natl Acad Sci U S A 1976;73:3608-3612.

21 Han SY, Chang EJ, Choi HJ, Kwak CS, Park SB, Kim HC, Mun KC: Apoptosis by cyclosporine in mesangial cells. Transplant Proc 2006;38:2244-2246.

22 Kitada N, Takara K, Itoh C, Minegaki T, Tsujimoto M, Sakaeda T, Yokoyama T: Comparative analysis of cell injury after exposure to antitumor platinum derivatives in kidney tubular epithelial cells. Chemotherapy 2008;54:217-223.

23 Ludwig T, Oberleithner H: Platinum complex toxicity in cultured renal epithelia. Cell Physiol Biochem 2004;14:431-440.

24 Sheikh-Hamad D, Cacini W, Buckley AR, Isaac J, Truong LD, Tsao CC, Kishore BK: Cellular and molecular studies on cisplatin-induced apoptotic cell death in rat kidney. Arch Toxicol 2004;78:147-155.

25 Lee RH, Song JM, Park MY, Kang SK, Kim YK, Jung JS: Cisplatin-induced apoptosis by translocation of endogenous Bax in mouse collecting duct cells. Biochem Pharmacol 2001;62:1013-1023.

26 Ishido M, Homma-Takeda S, Tohyama C, Suzuki T: Apoptosis in rat renal proximal tubular cells induced by cadmium. J Toxicol Environ Health A 1998;55:1-12.

27 Thevenod F: Nephrotoxicity and the proximal tubule. Insights from cadmium. Nephron Physiol 2003;93:p87-93.

28 Ye JL, Mao WP, Wu AL, Zhao JM, Zhang C, Zhang NN, Jiang P, Tian T: [Cadmium induced apoptosis of HEK293 cells and its mitochondrial apoptosis pathway]. Fen Zi Xi Bao Sheng Wu Xue Bao 2007;40:7-16.

29 L'Hoste S, Chargui A, Belfodil R, Duranton C, Rubera I, Mograbi B, Poujeol C, Tauc M, Poujeol P: CFTR mediates cadmium-induced apoptosis through modulation of ROS level in mouse proximal tubule cells. Free Radic Biol Med 2009;46:1017-1031.

30 Wang X, Takahashi N, Uramoto H, Okada Y: Chloride channel inhibition prevents ROS-dependent apoptosis induced by ischemia-reperfusion in mouse cardiomyocytes. Cell Physiol Biochem 2005;16:147-154.

31 Lang F, Gulbins E, Szabo I, Lepple-Wienhues A, Huber SM, Duranton C, Lang KS, Lang PA, Wieder T: Cell volume and the regulation of apoptotic cell death. J Mol Recognit 2004;17:473-480.

32 Lang F, Lepple-Wienhues A, Szabo I, Siemen D, Gulbins E: Cell volume in cell proliferation and apoptotic cell death. Contrib Nephrol 1998;123:158-168.

33 Bortner CD, Cidlowski JA: Cell shrinkage and monovalent cation fluxes: role in apoptosis. Arch Biochem Biophys 2007;462:176-188.

34 Krick S, Platoshyn O, Sweeney M, Kim H, Yuan JX: Activation of K+ channels induces apoptosis in vascular smooth muscle cells. Am J Physiol Cell Physiol 2001;280:C970-979.
35 Lee MP, Ravenel JD, Hu RJ, Lustig LR, Tomaselli G, Berger RD, Brandenburg SA, Litzi TJ, Bunton TE, Limb C, Francis H, Gorelikow M, Gu H, Washington K, Argani P, Goldenring JR, Coffey RJ, Feinberg AP: Targeted disruption of the Kvlqt1 gene causes deafness and gastric hyperplasia in mice. J Clin Invest 2000;106:1447-1455.
36 Demolombe S, Franco D, de Boer P, Kuperschmidt S, Roden D, Pereon Y, Jarry A, Moorman AF, Escande D: Differential expression of KvLQT1 and its regulator IsK in mouse epithelia. Am J Physiol Cell Physiol 2001;280:C359-372.
37 Zheng W, Verlander JW, Lynch IJ, Cash M, Shao J, Stow LR, Cain BD, Weiner ID, Wall SM, Wingo CS: Cellular distribution of the potassium channel KCNQ1 in normal mouse kidney. Am J Physiol Renal Physiol 2007;292:F456-466.
38 Barhanin J, Lesage F, Guillemare E, Fink M, Lazdunski M, Romey G: K(V)LQT1 and lsK (minK) proteins associate to form the I(Ks) cardiac potassium current. Nature 1996;384:78-80.
39 Wang Z, Li H, Moss AJ, Robinson J, Zareba W, Knilans T, Bowles NE, Towbin JA: Compound heterozygous mutations in KvLQT1 cause Jervell and Lange-Nielsen syndrome. Mol Genet Metab 2002;75:308-316.
40 Bendahhou S, Marionneau C, Haurogne K, Larroque MM, Derand R, Szuts V, Escande D, Demolombe S, Barhanin J: In vitro molecular interactions and distribution of KCNE family with KCNQ1 in the human heart. Cardiovasc Res 2005;67:529-538.
41 Schroeder BC, Waldegger S, Fehr S, Bleich M, Warth R, Greger R, Jentsch TJ: A constitutively open potassium channel formed by KCNQ1 and KCNE3. Nature 2000;403:196-199.
42 Grishin A, Ford H, Wang J, Li H, Salvador-Recatala V, Levitan ES, Zaks-Makhina E: Attenuation of apoptosis in enterocytes by blockade of potassium channels. Am J Physiol Gastrointest Liver Physiol 2005;289:G815-821.
43 Narumiya S, Sugimoto Y, Ushikubi F: Prostanoid receptors: structures, properties, and functions. Physiol Rev 1999;79:1193-1226.
44 Jensen BL, Stubbe J, Hansen PB, Andreasen D, Skott O: Localization of prostaglandin E(2) EP2 and EP4 receptors in the rat kidney. Am J Physiol Renal Physiol 2001;280:F1001-1009.